

# Chapter 8

## MR Based-Imaging Biomarkers in NAFLD/NASH



Michael Pavlides

### Introduction

Non-alcoholic fatty liver disease (NAFLD) is the most common cause of chronic liver disease in the Western World affecting up to a third of the adult population [1]. The disease varies in severity from accumulation of liver fat only (simple steatosis) to fat associated with inflammation (non-alcoholic steatohepatitis; NASH) and fibrosis and cirrhosis. It is now well established that patients with fibrosis are at increased risk of morbidity and mortality, while patients with simple steatosis generally have better prognosis [2, 3]. The prognostic importance of NASH remains a matter of debate [4].

The diagnostic classification of NAFLD into simple steatosis and NASH and the assessment of fibrosis relies on liver biopsy. This presents a challenge in clinical practice and in the conduct of clinical trials. In clinical practice, it is important to identify patients with high risk of morbidity/mortality from NAFLD so that they be prioritised for follow up in secondary care and for appropriate surveillance in cases of liver cirrhosis. As NAFLD is highly prevalent, liver biopsy is not practical as a diagnostic tool that needs to be applied at the level of the population, due to its, costs and invasiveness.

Liver biopsy and histological assessment of fibrosis and NASH are the only approved surrogate end points in clinical trials. Patients taking part in clinical trials therefore need to have repeated liver biopsies. Sampling errors and observer dependent variability in liver biopsy reporting means that more patients have to be recruited to achieve sufficient statistical power, while studies also suffer from high

---

M. Pavlides (✉)

Division of Cardiovascular Medicine, Radcliffe Department of Medicine,  
University of Oxford, Oxford, UK

Translational Gastroenterology Unit, Nuffield Department of Medicine, University of Oxford,  
Oxford, UK

Oxford NIHR Biomedical Research Centre, University of Oxford and Oxford University  
Hospitals NHS Foundation Trust, Oxford, UK  
e-mail: [michael.pavlides@cardiov.ox.ac.uk](mailto:michael.pavlides@cardiov.ox.ac.uk)

screening failure rates and dropouts. Presence of NASH and fibrosis are also important for inclusion into clinical trials.

Steatosis has traditionally been regarded as a “benign” feature in NAFLD that has no bearing on the progression of liver disease. This may be in part because steatosis is routinely quantified histologically as the “number of hepatocytes containing lipid droplets” which may not give an accurate estimate of the liver fat content. MRI on the other hand can quantify liver fat as a proportion (fat fraction; %) of liver tissue and is more accurate than histology [5]. In a natural history study, patients with liver fat fraction  $\geq 15.7\%$  as measured by MRI proton density fat fraction (PDFF) were more likely to progress their fibrosis than patients with fat fraction  $< 15.7\%$  were (multivariable adjusted odds ratio 6.7; 95% CI 1.01–44.1;  $p = 0.049$ ) [6].

Furthermore, evidence is emerging from clinical trials where liver fat is being assessed with MRI PDFF that suggests that reduction in liver fat is associated with histologic improvements. Data suggest that a relative decrease of 30% in liver fat is associated with improvements in NASH ( $\geq 2$  points reduction in the NAS score) [7–9] and steatosis on biopsy and serum markers of fibrosis and NASH activity [10–13]. Furthermore, the study of the fibroblast growth factor –19 analogue NGM282 produced a relative reduction in liver fat of 58% and 67% in those treated with 1 mg and 3 mg respectively and this was associated with improvement in fibrosis [14, 15].

In summary, there is an unmet need for non-invasive biomarkers of fibrosis as this is an important prognostic factor, for the diagnosis of NASH for inclusion in clinical trials and assessment of effectiveness and for steatosis that can be an early predictor of response to treatment. To address these areas of unmet clinical need and to reduce reliance on liver biopsy for the assessment of NAFLD in different contexts, several non-invasive techniques have been developed. These are generally divided into serum-based biomarkers (direct and indirect), ultrasound elastography based biomarkers and magnetic resonance based biomarkers, which will be the focus of this chapter. In general, simple indirect serum based markers are recommended for population screening in the community with direct serum markers [16] and transient elastography [17] reserved as a second tier of assessment. MR based biomarkers are generally reserved for cases where transient elastography fails [17].

Several MR biomarkers have been explored for several aspects of liver disease, focusing mainly on the distinction of NASH vs. non-NASH, the quantification of fibrosis, and for the monitoring of treatment response.

## Magnetic Resonance Elastography

### *Overview*

Magnetic Resonance Elastography (MRE; Resoundant, Rochester, US) is an MR technique that measures liver stiffness. Additional hardware and software is needed in order to carry out MRE and adaptations need to be made to the MR suite to accommodate these. During MRE, a plastic circular device is attached to the patient over the region of the liver. Mechanically generated shear waves are transmitted

through the circular device to the liver and their propagation is visualised using specific MR sequences (e.g. 2D-gradient recalled echo (GRE) pulse sequences). These data are then used to provide an estimate of the liver stiffness, which is mostly considered a biomarker of fibrosis. 2D-MRE is clinically available and is the most validated of the MR based biomarkers in NAFLD having been tested in approximately 700 patients. 3D-MRE is also in development and this has also been explored in the assessment of patients with NAFLD. 3D-MRE gives information additional to stiffness and early studies show that it may result in improved performance.

MRE has a low failure rate (4.3%) [18] and excellent inter-observer agreement (intraclass correlation coefficient 0.95) [19].

### ***NASH vs. Non NASH***

In a retrospective study the area under the receiver operating curve (AUROC) of 2D MRE for the diagnosis of NASH was reported as 0.93 [20] (threshold 2.74 kPa, Se 0.94, Sp 0.73, PPV 0.85, NPV 0.89; Threshold 2.90 kPa Se 0.83, Sp 0.82, PPV 0.88, NPV 0.75). However, this level of performance was not replicated in five prospective studies that reported area under the curve (AUC) ranging from 0.70 to 0.81 [21–25]. Furthermore, these studies report on the best thresholds derived on their population. There is therefore no prospective validation on the performance of pre-defined cut-offs. MRE does not offer any improvement in the diagnosis of NASH compared to transient elastography [22, 25].

Studies that have examined 3D MRE for the diagnosis of NASH have also reported only moderate diagnostic accuracy. In a study of 100 patients 3D MRE (60 Hz) and 3D MRE (40 Hz) had AUROC of 0.76 and 0.74 respectively, compared to 2D MRE (60 Hz) of 0.75 [23]. In patients who were undergoing bariatric surgery, the AUROC for the diagnosis of NASH was 0.73 and for the evaluation of disease activity using the NAS score was 0.82 [26].

### ***Staging of Fibrosis in NAFLD***

The performance of MRE for the assessment of fibrosis has been the subject of meta-analysis. In a meta-analysis of 5 studies including 628 patients, the mean AUC of the pooled data for the diagnosis of significant fibrosis ( $F \geq 2$ ), advanced fibrosis ( $\geq 3$ ) and cirrhosis were 0.88 (95% CI 0.83–0.92), 0.93 (0.90–0.97) and 0.92 (0.80–1.00) respectively. In an individual patient data meta-analysis of 115 patients from eight studies, the AUC for the diagnosis of fibrosis stage  $\geq 1$ ,  $\geq 2$ ,  $\geq 3$ , and 4 were 0.89 (0.81–0.97), 0.90 (0.79–0.93), 0.94 (0.91–0.98) and 0.90 (0.64–0.94) respectively. MRE performed better than TE in a comparative individual patient data meta-analysis of 230 patients [27]. 2D MRE also performs better than serum based indirect biomarkers [28]. Data on diagnostic performance of MRE in selected individual studies are shown in Table 8.1.

**Table 8.1** Diagnostic performance of magnetic resonance elastography for the assessment of fibrosis in patients with non-alcoholic fatty liver disease

Study	Study design	Population and prevalence of fibrosis stages	Diagnostic performance
Kim 2013 [29]	Retrospective 2D MRE	142 patients with NAFLD F0 = 50, F1 = 34, F2 = 12, F3 = 10, F4 = 36	AUC = 0.95 for F ≥ 3
Loomba 2014 [24]	Prospective 2D MRE	117 patients with NAFLD F0 = 43, F1 = 39, F2 = 13, F3 = 12, F4 = 10	AUC = 0.84 for F ≥ 1 AUC = 0.86 for F ≥ 2 AUC = 0.92 for F ≥ 3 AUC = 0.89 for F4
Cui 2016 [30]	Prospective 2D MRE	125 patients with NAFLD F0 = 53, F1 = 39, F2 = 12, F3 = 12, F4 = 9	AUC = 0.80 for F ≥ 1 AUC = 0.89 for F ≥ 2 AUC = 0.93 for F ≥ 3 AUC = 0.88 for F4
Imajo 2016 [22]	Prospective 2D MRE	142 patients with NAFLD F0 = 14, F1 = 51, F2 = 32, F3 = 34, F4 = 11	AUC = 0.80 for F ≥ 1 AUC = 0.89 for F ≥ 2 AUC = 0.89 for F ≥ 3 AUC = 0.97 for F4
Loomba 2016 [23]	Prospective 2D MRE (60 Hz)	100 patients with NAFLD F0 = 41, F1 = 32, F2 = 12, F3 = 10, F4 = 5	AUC = 0.85 for F ≥ 1 AUC = 0.88 for F ≥ 2 AUC = 0.92 for F ≥ 3 AUC = 0.98 for F4
	3D MRE (60 Hz)		AUC = 0.86 for F ≥ 1 AUC = 0.84 for F ≥ 2 AUC = 0.93 for F ≥ 3 AUC = 0.98 for F4
	3D MRE (40 Hz)		AUC = 0.85 for F ≥ 1 AUC = 0.86 for F ≥ 2 AUC = 0.98 for F ≥ 3 AUC = 0.99 for F4
Park 2017 [25]	Prospective 2D MRE	104 patients with NAFLD F0 = 47, F1 = 24, F2 = 11, F3 = 13, F4 = 8	AUC = 0.82 for F ≥ 1 AUC = 0.89 for F ≥ 2 AUC = 0.87 for F ≥ 3 AUC = 0.87 for F4
Costa-Silva 2018 [21]	Prospective 2D MRE	49 patients with NAFLD F0 = 21, F1 = 16, F2 = 1, F3 = 8, F4 = 3	AUC = 0.88 for F ≥ 1 AUC = 0.93 for F ≥ 2 AUC = 0.93 for F ≥ 3 AUC = 0.96 for F4

Abbreviations: 2D MRE 2 dimensional magnetic resonance elastography, NAFLD non-alcoholic fatty liver disease, AUC area under the curve

### Monitoring Treatment Response

MRE has been validated as an exploratory end point in several clinical trials. In an analysis of the data from the phase II trial of selonsertib [31], MRE had an AUC of 0.62 (95% CI: 0.46–0.78) for the prediction of fibrosis improvement, and an

AUC of 0.57 (95% CI of 0.36–0.79 for the prediction of fibrosis progression [32]. In another secondary analysis of the placebo arms of two clinical trials [7, 33], a decrease of  $\geq 5\%$  in body mass index, was associated with a decrease in MRE liver stiffness, while patients who did not lose weight did not show any MRE changes [34].

## *Predicting Adverse Clinical Outcomes*

There are no studies looking at the predictive value of MRE in patients with NAFLD. In a retrospective study of patients with advanced fibrosis (25% had NAFLD), MRE liver stiffness predicted decompensation independently of age, MELD score, serum albumin and hepatitis C diagnosis [35].

## **LiverMultiScan™**

### *Overview*

LiverMultiScan™ (LMS; Perspectum Diagnostics, Oxford, UK) uses multiple MRI parameters (shMOLLI T1 mapping, T2\* and PDFF) to provide quantitative measures of liver fibrosis and inflammation, fat and iron. Central to this technology is the correction of the T1 relaxation time, as measured by the shMOLLI technique [36], for iron. T1 is an inherent property of tissues that can change with varying fibrosis and inflammation. T1 is however confounded by the presence of iron. In LMS, the measured T1 is corrected for the amount of iron present (as measured by T2\*), to produce the “iron corrected T1 (cT1)”, something that improves the diagnostic accuracy [37]. Even though, this technique has not been validated to the same extent as MRE in patients with NAFLD, it is being used as part of the abdominal imaging protocol in the UK Biobank study [38–41], something that makes it by far the most validated technique in terms of total participants scanned and whose data were subsequently published. Figure 8.1 illustrates this technique in a patient who has undergone bariatric surgery.

The failure rate of LMS is very low (2–5%) [42, 43] in clinical studies. The main reasons for failed scans are participant related factors (e.g. claustrophobia). The failure rate remains at the same low levels when LMS is used in population level studies [38, 39]. LMS cT1 is also a robust technique with excellent reproducibility across scanners and magnet strengths (coefficient of variance 3.3%, bias 6.5 ms, 95% Level of agreement: –76.3 to 89.2 ms) and scan-rescan repeatability (coefficient of variance 1.7%, bias –7.5 ms, 95% Level of agreement: –53.6 to 38.5 ms) [44]. In head to head comparison LMS had superior test re-test repeatability compared to MR elastography and transient elastography [45].

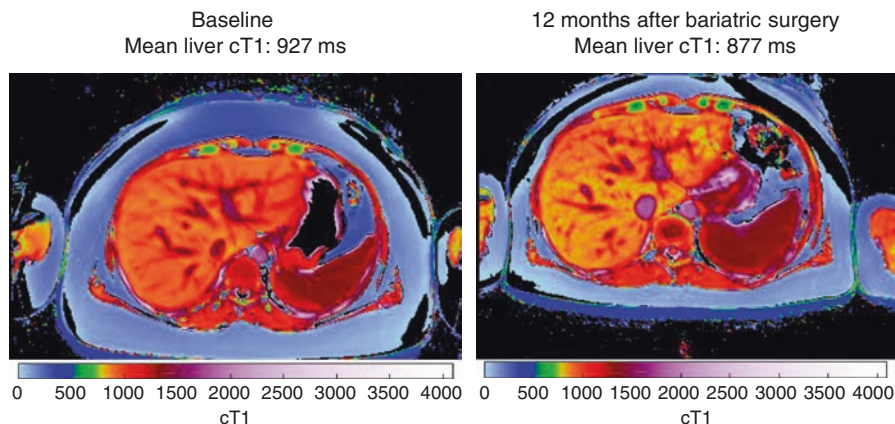


**Fig. 8.1** Liver *Multiscan* iron corrected T1 maps. Liver *Multiscan* produces iron corrected T1 maps that can be used to measure mean cT1. The figure illustrates how the technique can be used to measure change in cT1 after therapeutic intervention, like bariatric surgery

### *NASH vs. Non-NASH and Staging of NAFLD Fibrosis*

Two studies have examined the value of LMS in the staging of fibrosis and the identification of NASH compared to liver biopsy. In a study of 71 patients from one centre [46], LMS cT1 had an excellent diagnostic accuracy for the identification of significant NAFLD as defined by the FLIP consortium algorithm [47] (AUROC 0.89), while there was good performance for the differentiation of NASH vs. simple steatosis (AUROC 0.80). Furthermore, LMS cT1 could identify patients with significant activity (ballooning + lobular inflammation; AUROC 0.83) and cirrhosis (AUROC 0.85). In a two centre study of 50 patients [48], LMS cT1 had moderate diagnostic performance for the separation of NASH vs. simple steatosis (AUROC 0.69), but it must be noted that a different definition of NASH [49] was used in this study. Even though LMS cT1 did not perform as well for the diagnosis of fibrosis compared to alternative tests, it had the highest negative predictive value for the exclusion of significant disease where biopsy could be avoided, and an algorithm in combination with transient elastography had the lowest cost per correct diagnosis [48].

### *Monitoring Treatment Response*

In a study of an engineered fibroblast growth factor 19 analogue (NGM282), both LMS cT1 and PDFF decreased as early as 6 weeks after treatment indicating that this method could be used to assess effectiveness at early time points. This can

improve the design and conduct of clinical trials. LMS cT1 has also been used as a primary end-point in a study without histologic verification of effectiveness, that showed no therapeutic benefit of the investigational product [45]. Along with LMS cT1, there was no improvement in MRE or TE or liver fat measured by LMS PDFF.

### ***Predicting Adverse Clinical Outcomes***

LMS has not been specifically tested for the prediction of clinical outcomes in cohorts of patients with NAFLD. In a study including patients with mixed aetiologies (35% NAFLD) and varying degrees of fibrosis, LMS cT1 had a hazard ratio of 9.7 for the prediction of liver related events [50]. In the same study, a model including all three LMS variables (cT1, T2\* and PDFF) had a hazard ratio of 75.7 demonstrating how the multi-parameter approach in this test can provide improved performance.

It should also be noted that liver T1 was found to correlate with heart failure, atrial fibrillation, and coronary heart disease in the Multi-Ethnic Study of Atherosclerosis [51]. This is important, as it is well documented that cardiovascular disease is the main cause of mortality in patients with NAFLD [2, 3].

## **Detection of Metabolic Liver Injury (deMILI) MRI**

### ***Overview***

Detection of metabolic liver injury (deMILI) MRI uses optical analysis of magnetic resonance images to define NASHMRI (0-1) and FibroMRI (0-1), measures of NASH and liver fibrosis respectively. Image acquisition does not require injection of intravenous contrast and include SSFSE-T2 (Single Shot Fast Spin Echo T2-weighted), FAST-STIR (Fast Short inversion Time Inversion Recovery), inPHASE-outPHASE (in and out Phase) and DYNAMIC [52]. Figure 8.2 illustrates the imaging processing and the report for NASHMRI and FibroMRI.

This technique has been validated on 1.5T Phillips and General Electric scanners. Available data suggest that the between scanner reproducibility is good when tested using independent cohorts in Phillips and GE scanners [52]. In small number of patients (n = 9) assessed by both Philips and GE scanners, FibroMRI correctly detected in fibrosis in 3/3 cases and correctly excluded in 5/6 cases using both Philips and GE devices. Furthermore, NASH was correctly diagnosed in 3/4 cases and correctly excluded in 4/5 cases using NASHMRI on data from both scanners [52].



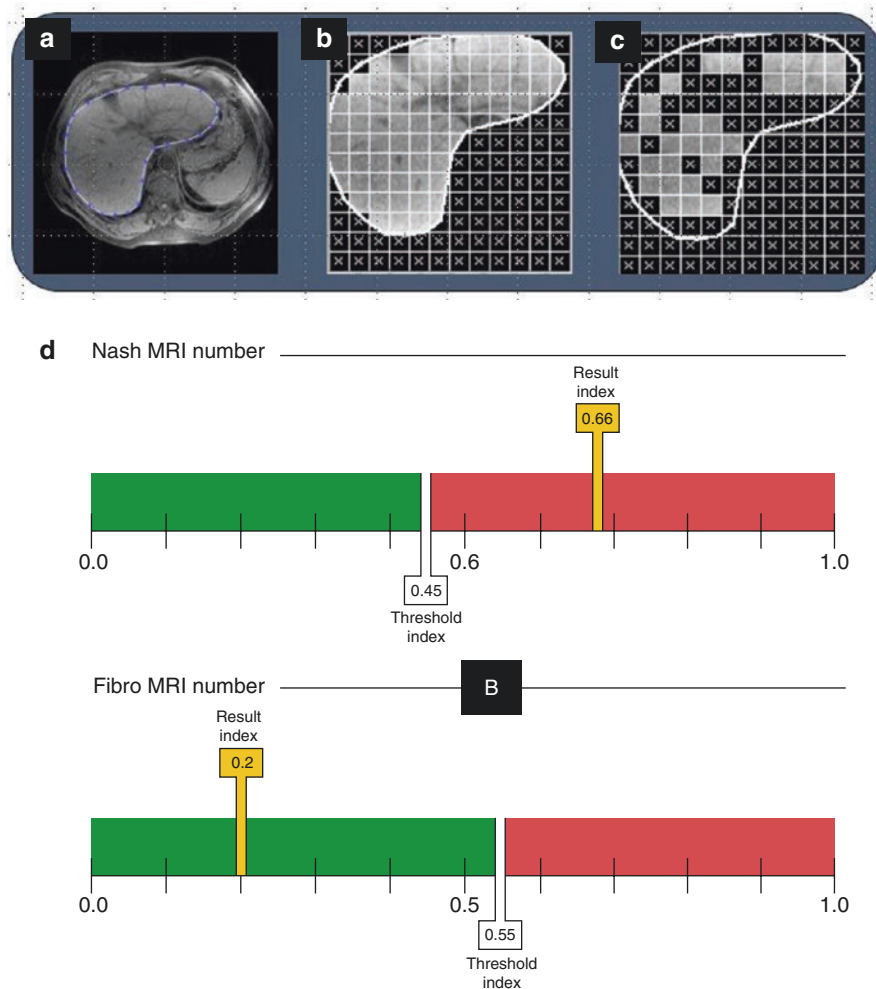


**Fig. 8.2** DeMILI image processing and report. The deMILI image processing includes steps for (a) the manual outlining of the liver boundary, (b) segmentation and overlapping of a grid, (c) a process for selection of valid regions of interest. (d) The final report is presented as NASHMRI (0-1) where a score above 0.5 indicates NASH and FibroMRI (0-1) where a score above 0.5 indicates significant fibrosis

### *NASH vs. Non-NASH and Staging of NAFLD Fibrosis*

In a prospective study, NASHMRI and FibroMRI were defined based on the most predictive parameters in an estimation and validation cohorts. For the diagnosis of NASH, that was defined histologically based on the overall distribution of lesions especially lobular inflammation and ballooning, NASHMRI had an AUROC of 0.88 (best cut-off 0.5, sensitivity (Se) 0.87, specificity (Sp) 0.74, positive predictive value



(PPV): 0.8, negative predictive value (NPV): 0.82) in the estimation cohort and 0.83 (cut-off 0.5, Se 0.87, Sp 0.6, PPV 0.71, NPV 0.81) in the validation cohort. NASHMRI performed better than Cytokeratin 18 (CK-18) for the diagnosis of NASH [52].

For the diagnosis of significant fibrosis, (F0-F1 vs. F2-F4) FibroMRI had an AUROC of 0.94 (cut-off 0.5, Se 0.81, Sp 0.85, PPV 0.77 and NPV 0.86) in the estimation cohort and 0.85 (cut-off 0.5, Se 0.77, Sp 0.80, PPV 0.67, and NPV 0.87) in the validation cohort. FibroMRI had superior performance compared to serum based fibrosis scores, and similar performance to transient elastography [52].

## Dynamic Contrast Enhanced MRI

### *Overview*

Dynamic contrast enhanced MRI relies on the MR signal change in tissues after the injection of intravenous contrast agents. Several contrast agents are available. For the assessment of chronic liver disease, gadoteric acid is preferred as the liver actively excretes it in bile. In these scans, gadoteric acid is injected intravenously after acquisition of baseline data. Scans are then acquired at different time points to reflect how the contrast is distributed at the arterial and portal venous phases. Gadoteric acid is actively taken up by liver cells and then it is selectively excreted into bile. Transmembrane transporters control uptake and excretion. The number of liver cells and their summative level of function ultimately determines how much contrast is taken up into and secreted from the liver. This can be assessed by measuring the resultant change in signal intensity in the liver. Figure 8.3 illustrates how the decrease in signal intensity (T1 in this case) can be used to distinguish normal liver from diseased livers.

This technique requires the injection of intravenous contrast, which is contraindicated in patients with significant renal dysfunction. The advantage of this technique is that it can be applied across scanners and magnet strengths. As it is assessing relative change it requires no further standardisation to make it applicable between scanners. Most of the validation of this technique has been carried out in retrospective studies of patients who were having MR scans as part of their clinical care, so applicability to the wider NAFLD population has not been assessed.

### *NASH vs. Non-NASH and Staging of NAFLD Fibrosis*

There have been some studies showing utility of this technique in animal models of NAFLD/NASH [53–55]. A retrospective human study of 81 patients showed that the relative signal enhancement after contrast injection was associated with lobular inflammation ( $p = 0.002$ ), ballooning ( $p = 0.04$ ) and fibrosis ( $p < 0.0001$ ) but

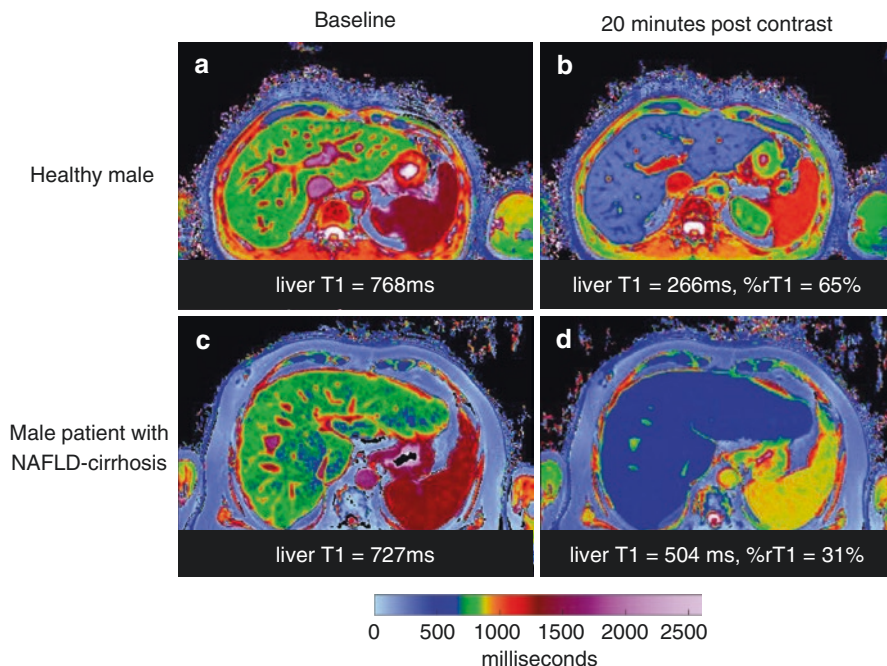


**Fig. 8.3** Gadoteric acid enhanced MRI. The relative reduction in T1 20 min after gadoteric acid injection in a healthy male and patient with cirrhosis from non-alcoholic fatty liver disease (NAFLD). In the healthy male, T1 decreases from (a) baseline of 768 ms to a (b) post contrast T1 of 266 ms, a relative reduction (percentagerT1) of 65%, while in the case of the patient, the T1 decreases from (c) a baseline of 727 ms to a (d) post contrast T1 of 504 ms, a relative reduction of 31%

not with steatosis ( $p = 0.38$ ) [56]. For the diagnosis of NASH as defined by the Steatosis Activity Fibrosis (SAF) classification [47], this technique had an AUC of 0.85 (threshold 1.24, Se 0.97, Sp 0.63).

Several studies have assessed DCE MRI in mixed cohorts of patients showing some utility in the assessment of liver fibrosis [57], cirrhosis severity [58–60], and liver function [60, 61], including some studies showing superior performance of DCE MRI for the assessment of fibrosis compared to unenhanced T1 and diffusion weighted imaging [62, 63]. However, generalisation of these results to NAFLD patients must not be assumed.

A related approach to using gadolinium based contrast agents is to use iron containing contrast agents. Superparamagnetic iron oxide particles have been tested, but these have since been taken off the market [64]. More recently, there has been some interest in ultrasmall superparamagnetic iron oxide particles. The iron containing contrast leads to changes in tissue  $R2^*$  which can be measured. In a small, prospective, proof-of-concept study, the AUC for the diagnosis of NASH vs. simple steatosis was 0.87 (95% CI 0.72–1.0) [65]. However, the post contrast scans are acquired 72 h after injection something that is impractical in clinical practice.

## Diffusion Weighted Imaging

### *Overview*

Diffusion weighted imaging (DWI) uses MRI acquisition and analysis techniques to track diffusion of water in tissues. Quantitative measures of diffusion can be produced by measuring the magnitude (apparent diffusion coefficient; ADC) and directionality (fractional anisotropy) of diffusion. The accumulation of steatosis, inflammation and fibrosis can lead to changes in water diffusion and these can be measured using various DWI techniques. Intravoxel incoherent motion (IVIM) is a DWI method that can account for the diffusion signal contributed from blood flowing in vascular beds [66].

The failure rate of this technique was up to 17.5% in one study [67]. The method of analysis can also have a significant impact on results [68].

### *NASH vs. Non-NASH and Staging of NAFLD Fibrosis*

A study of 59 patients with type 2 diabetes mellitus and NAFLD evaluated the IVIM parameters of “pure molecular diffusion;  $D$ ”, “perfusion related diffusion,  $D^*$  and “perfusion fraction;  $f$ ”. The study found only moderate diagnostic accuracy for the diagnosis of NASH (AUC 0.74 for  $D$ , 0.68 for  $D^*$ , 0.61 for  $f$ ) and fibrosis (AUC 0.69 for  $D$ , 0.68 for  $D^*$ , 0.62 for  $f$ ) [67]. In a separate study of 89 patients with NAFLD, steatosis and fibrosis had significant and independent effects on  $D$  and  $f$  [68]. The effects of steatosis have also been observed in other studies [69–72].

In an interesting retrospective study of 15 patients (only 2 with NAFLD), a method is proposed by which IVIM can be used to generate a “virtual elastogram” based on a calibrated relationship between ADC and liver elasticity [73]. This lacks prospective validation in patients with NAFLD but could provide an added advantage to MRE as it could potentially produce equivalent data without the need for additional hardware.

## Conclusions

The field of MR based biomarkers is relatively new compared to serum-based biomarkers and ultrasound based elastography techniques. Of the techniques that have been reviewed in this chapter, MRE (+PDFF for fat) and LMS have had most validation in NAFLD and they show promise for further clinical utility. MRE has the best performance for assessment of late stages of fibrosis. PDFF for liver fat content quantification is emerging as an important parameter for predicting histological response.

How various MR techniques are utilised in clinical pathways and clinical trials remains to be determined. Current recommendations [17] favour application of MR based techniques as a third tier of non-invasive tests after serum based and ultrasound elastography. While this approach may be more practical there are no cost effectiveness data to support it and it could be that application of MR based techniques “up-front” are more cost effective if they have superior diagnostic accuracy.

One other area that needs further attention is the validation of pre-defined thresholds to be used in different situations (contexts of use). For example, there is growing evidence that a relative reduction of 30% in liver fat content predicts histological response but data are still lacking on prospective validation of predefined cut-offs for varying fibrosis severities. Data on the prognostic value of MR based biomarkers in NAFLD cohorts are also needed.

MR based biomarkers will certainly have a role in the assessment of patients with NAFLD as the data reviewed here demonstrate advantages in some key areas beyond diagnostic accuracy. MR based biomarkers are robust with excellent reproducibility and repeatability, can be applied at population level as in the case of Liver *Multiscan* being used in the UK Biobank imaging study. Further technical improvements are also possible as in the use of diffusion weighted imaging to perform “virtual elastography”.

**Acknowledgements** I would like to thank Mr. Arjun Jayaswal for providing the Liver Multiscan images in Fig. 8.1, Prof. Manuel Romero-Gomez for providing the deMILI images in Fig. 8.2, and Dr. Christina Levick for providing the images for Fig. 8.3.

## References

1. Wong VW, Chu WC, Wong GL, Chan RS, Chim AM, Ong A, et al. Prevalence of non-alcoholic fatty liver disease and advanced fibrosis in Hong Kong Chinese: a population study using proton-magnetic resonance spectroscopy and transient elastography. *Gut*. 2012;61(3):409–15.
2. Angulo P, Kleiner DE, Dam-Larsen S, Adams LA, Bjornsson ES, Charatcharoenwitthaya P, et al. Liver fibrosis, but no other histologic features, is associated with long-term outcomes of patients with nonalcoholic fatty liver disease. *Gastroenterology*. 2015;149(2):389–97.e10.
3. Ekstedt M, Hagstrom H, Nasr P, Fredrikson M, Stal P, Kechagias S, et al. Fibrosis stage is the strongest predictor for disease-specific mortality in NAFLD after up to 33 years of follow-up. *Hepatology (Baltimore, Md)*. 2015;61(5):1547–54.
4. Ratzl V. Back to Byzance: querelles byzantines over NASH and fibrosis. *J Hepatol*. 2017;67(6):1134–6.
5. Raptis DA, Fischer MA, Graf R, Nanz D, Weber A, Moritz W, et al. MRI: the new reference standard in quantifying hepatic steatosis? *Gut*. 2012;61(1):117–27.
6. Ajmera V, Park CC, Caussy C, Singh S, Hernandez C, Bettencourt R, et al. Magnetic resonance imaging proton density fat fraction associates with progression of fibrosis in patients with non-alcoholic fatty liver disease. *Gastroenterology*. 2018;155(2):307–10. e2
7. Loomba R, Sirlin CB, Ang B, Bettencourt R, Jain R, Salotti J, et al. Ezetimibe for the treatment of nonalcoholic steatohepatitis: assessment by novel magnetic resonance imaging and magnetic resonance elastography in a randomized trial (MOZART trial). *Hepatology (Baltimore, Md)*. 2015;61(4):1239–50.

8. Loomba R, Neuschwander-Tetri BA, Sanyal AJ, Chalasani NP, Diehl AM, Terrault N, et al. Novel multicenter validation of association between decline in MRI-PDFF and histologic response: a secondary analysis of FLINT trial. *Hepatology* (Baltimore, Md). 2017;66.
9. Neuschwander-Tetri BA, Loomba R, Sanyal AJ, Lavine JE, Van Natta ML, Abdelmalek MF, et al. Farnesoid X nuclear receptor ligand obeticholic acid for non-cirrhotic, non-alcoholic steatohepatitis (FLINT): a multicentre, randomised, placebo-controlled trial. *Lancet*. 2015;385(9972):956–65.
10. Loomba R, Lawitz E, Mantry PS, Jayakumar S, Caldwell SH, Arnold H, et al. GS-4997, an Inhibitor of apoptosis signal-regulating kinase (ASK1), alone or in combination with simtuzumab for the treatment of nonalcoholic steatohepatitis (nash): a randomized, phase 2 trial. *Hepatology* (Baltimore, Md). 2016;64(6).
11. Loomba R, Lawitz E, Ghalib R, Elkhashab M, Caldwell S, Abdelmalek M, et al. Longitudinal changes in liver stiffness by magnetic resonance elastography (MRE), liver fibrosis, and serum markers of fibrosis in a multi-center clinical trial in nonalcoholic steatohepatitis (NASH). *J Hepatol*. 2017;66(1):S671.
12. Artwick E, Luo Y, Christian R, Sanyal A, Charles E, Tetri BN, et al. BMS-986036 (pegylated FGF21) in patients with non-alcoholic steatohepatitis: a phase 2 study. *Hepatology international Conference: 27th asian pacific association for the study of the liver, APASL 2018 India*. 2018;12(2):S231-S2.
13. Charles ED, Dong Y, Gagnon RC, Luo Y, Du S, Christian R, et al. Multi-biomarker validation of MRI-pdffand mre-derived treatment response with BMS-986036 (PEG-FGF21): a secondary analysis of a multi-center clinical trial in non-alcoholic steatohepatitis (NASH). *Hepatology* (Baltimore, Md). 2017;66.
14. Harrison SA, Rinella ME, Abdelmalek MF, Trotter JF, Paredes AH, Arnold HL, et al. NGM282 for treatment of non-alcoholic steatohepatitis: a multicentre, randomised, double-blind, placebo-controlled, phase 2 trial. *Lancet*. 2018;391(10126):1174–85.
15. Harrison SA, Rossi SJ, Paredes AH, Trotter JF, Bashir MR, Guy CD, et al. NGM282 improves liver fibrosis and histology in 12 weeks in patients with nonalcoholic steatohepatitis. *Hepatology* (Baltimore, Md) 2019. <https://doi.org/10.1002/hep.30590>. [Epub ahead of print].
16. Srivastava A, Gailer R, Tanwar S, Trembling P, Parkes J, Rodger A, et al. Prospective evaluation of a primary care referral pathway for patients with non-alcoholic fatty liver disease. *J Hepatol*. 2019;71(2):371–8.
17. Castera L, Friedrich-Rust M, Loomba R. Noninvasive assessment of liver disease in patients with nonalcoholic fatty liver disease. *Gastroenterology*. 2019;156(5):1264–81.e4.
18. Singh J, Garg A, Sahney A, Mazumder S, Vij JC, Batra Y, et al. Comparison of non-invasive methods to diagnose non-alcoholic fatty liver disease in morbidly obese patients undergoing bariatric surgery. *Indian J Gastroenterol*. 2017;36(1).
19. Chen J, Yin M, Talwalkar JA, Oudry J, Glaser KJ, Smyrk TC, et al. Diagnostic performance of MR elastography and vibration-controlled transient elastography in the detection of hepatic fibrosis in patients with severe to morbid obesity. *Radiology*. 2017;283(2):418–28.
20. Chen J, Talwalkar JA, Yin M, Glaser KJ, Sanderson SO, Ehman RL. Early detection of nonalcoholic steatohepatitis in patients with nonalcoholic fatty liver disease by using MR elastography. *Radiology*. 2011;259(3):749–56.
21. Costa-Silva L, Ferolla SM, Lima AS, Vidigal PVT, Ferrari TCA. MR elastography is effective for the non-invasive evaluation of fibrosis and necroinflammatory activity in patients with nonalcoholic fatty liver disease. *Eur J Radiol*. 2018;98:82–9.
22. Imajo K, Kessoku T, Honda Y, Tomeno W, Ogawa Y, Mawatari H, et al. Magnetic resonance imaging more accurately classifies steatosis and fibrosis in patients with nonalcoholic fatty liver disease than transient elastography. *Gastroenterology*. 2016;150(3):626–37.e7. <http://onlinelibrary.wiley.com/doi/10.1016/j.gastro.2016.01.011>
23. Loomba R, Cui J, Wolfson T, Haufe W, Hooker J, Szevenyi N, et al. Novel 3D magnetic resonance elastography for the noninvasive diagnosis of advanced fibrosis in NAFLD: a prospective study. *Am J Gastroenterol*. 2016;111(7):986–94.

24. Loomba R, Wolfson T, Ang B, Hooker J, Behling C, Peterson M, et al. Magnetic resonance elastography predicts advanced fibrosis in patients with nonalcoholic fatty liver disease: a prospective study. *Hepatology* (Baltimore, Md). 2014;60(6):1920–8.
25. Park CC, Nguyen P, Hernandez C, Bettencourt R, Ramirez KS, Fortney LE, et al. Magnetic resonance elastography vs. transient elastography in detection of fibrosis and noninvasive measurement of steatosis in patients with biopsy-proven nonalcoholic fatty liver disease. *J Hepatol*. 2017;66(1).
26. Allen AM, Shah VH, Therneau TM, Venkatesh SK, Mounajjed T, Larson JJ, et al. The role of three-dimensional magnetic resonance elastography in the diagnosis of nonalcoholic steatohepatitis in obese patients undergoing bariatric surgery. *Hepatology* (Baltimore, Md). 2018. <https://doi.org/10.1002/hep.30483>. [Epub ahead of print].
27. Hsu C, Caussy C, Imajo K, Chen J, Singh S, Kaulback K, et al. Magnetic resonance vs transient elastography analysis of patients with nonalcoholic fatty liver disease: a systematic review and pooled analysis of individual participants. *Clin Gastroenterol Hepatol*. 2019;17(4):630–7.e8.
28. Cui J, Ang B, Haufe W, Hernandez C, Verna EC, Sirlin CB, et al. Comparative diagnostic accuracy of magnetic resonance elastography vs. eight clinical prediction rules for non-invasive diagnosis of advanced fibrosis in biopsy-proven non-alcoholic fatty liver disease: a prospective study. *Aliment Pharmacol Ther*. 2015;41(12):1271–80.
29. Kim D, Kim WR, Talwalkar JA, Kim HJ, Ehman RL. Advanced fibrosis in nonalcoholic fatty liver disease: noninvasive assessment with MR elastography. *Radiology*. 2013;268(2):411–9.
30. Cui J, Heba E, Hernandez C, Haufe W, Hooker J, Andre MP, et al. Magnetic resonance elastography is superior to acoustic radiation force impulse for the diagnosis of fibrosis in patients with biopsy-proven nonalcoholic fatty liver disease: a prospective study. *Hepatology* (Baltimore, Md). 2016;63(2):453–61.
31. Loomba R, Lawitz E, Mantry PS, Jayakumar S, Caldwell SH, Arnold H, et al. The ASK1 inhibitor selonsertib in patients with nonalcoholic steatohepatitis: a randomized, phase 2 trial. *Hepatology* (Baltimore, Md). 2018;67(2):549–59.
32. Jayakumar S, Middleton MS, Lawitz EJ, Mantry PS, Caldwell SH, Arnold H, et al. Longitudinal correlations between MRE, MRI-PDFF, and liver histology in patients with non-alcoholic steatohepatitis: analysis of data from a phase II trial of selonsertib. *J Hepatol*. 2019;70(1):133–41.
33. Cui J, Philo L, Nguyen P, Hofflich H, Hernandez C, Bettencourt R, et al. Sitagliptin vs. placebo for non-alcoholic fatty liver disease: a randomized controlled trial. *J Hepatol*. 2016;65(2):369–76.
34. Patel N, Doycheva I, Peterson M, Hooker J, Kisselva T, Schnabl B, et al. Effect of weight loss on magnetic resonance imaging estimation of liver fat and volume in patients with nonalcoholic steatohepatitis. *Clin Gastroenterol Hepatol*. 2015;13(3):561–8.e1. <http://onlinelibrary.wiley.com/doi/10.1016/j.cgh.2015.01.011>
35. Asrani SK, Talwalkar JA, Kamath PS, Shah VH, Saracino G, Jennings L, et al. Role of magnetic resonance elastography in compensated and decompensated liver disease. *J Hepatol*. 2014;60(5):934–9.
36. Piechnik SK, Ferreira VM, Dall'Armellina E, Cochlin LE, Greiser A, Neubauer S, et al. Shortened Modified Look-Locker Inversion recovery (ShMOLLI) for clinical myocardial T1-mapping at 1.5 and 3 T within a 9 heartbeat breathhold. *J Cardiovasc Magn Reson*. 2010;12:69.
37. Tunnicliffe EM, Banerjee R, Pavlides M, Neubauer S, Robson MD. A model for hepatic fibrosis: the competing effects of cell loss and iron on shortened modified Look-Locker inversion recovery T1 (shMOLLI-T1) in the liver. *J Magn Reson Imaging*. 2017;45(2):450–62.
38. McKay A, Wilman HR, Dennis A, Kelly M, Gyngell ML, Neubauer S, et al. Measurement of liver iron by magnetic resonance imaging in the UK Biobank population. *PLoS One*. 2018;13(12):e0209340.



39. Mojtahed A, Kelly CJ, Herlihy AH, Kin S, Wilman HR, McKay A, et al. Reference range of liver corrected T1 values in a population at low risk for fatty liver disease—a UK Biobank sub-study, with an appendix of interesting cases. *Abdom Radiol (NY)*. 2019;44(1):72–84.
40. Triay Bagur A, Hutton C, Irving B, Gyngell ML, Robson MD, Brady M. Magnitude-intrinsic water-fat ambiguity can be resolved with multipeak fat modeling and a multipoint search method. *Magn Reson Med*. 2019;82:460–75.
41. Wilman HR, Kelly M, Milanese M, Herlihy A, Gyngell M, Neubauer S, et al. Characterisation of liver fat in the UK Biobank cohort. *PLoS One*. 2017;12(2):e0172921.
42. Pavlides M, Banerjee R, Tunnicliffe EM, Kelly C, Collier J, Wang LM, et al. Multiparametric magnetic resonance imaging for the assessment of non-alcoholic fatty liver disease severity. *Liver Int*. 2017;37(7):1065–73.
43. Banerjee R, Pavlides M, Tunnicliffe EM, Piechnik SK, Schneider JE, Robson MD, et al. Multiparametric magnetic resonance for the non-invasive diagnosis of liver disease. *J Hepatol*. 2014;60(1):69–77.
44. Bachtiar V, Kelly MD, Wilman HR, Jacobs J, Newbould R, Kelly CJ, et al. Repeatability and reproducibility of multiparametric magnetic resonance imaging of the liver. *PLoS One*. 2019;14(4):e0214921.
45. Harrison SA, Neubauer S, Dennis A, Fiore MM, Kelly MD, Kelly CJ, et al. Utility and variability of three non-invasive liver fibrosis imaging modalities to evaluate efficacy of GR-MD-02 in subjects with NASH and bridging fibrosis during a phase-2 randomized clinical trial. *PLoS One*. 2018;13(9):e0203054.
46. Pavlides M, Tunnicliffe EM, Robson MD, Neubauer S, Collier J, Cobbold JF, et al. Multiparametric magnetic resonance imaging for the assessment of non-alcoholic fatty liver disease severity. *Liver Int*. 2017;37(7):1065–73.
47. Bedossa P. Utility and appropriateness of the fatty liver inhibition of progression (FLIP) algorithm and steatosis, activity, and fibrosis (SAF) score in the evaluation of biopsies of nonalcoholic fatty liver disease. *Hepatology (Baltimore, Md)*. 2014;60(2):565–75.
48. Eddowes PJ, Davies N, Hodson J, Newsome PN, Flintham RB, Wesolowski R, et al. Utility and cost evaluation of multiparametric magnetic resonance imaging for the assessment of non-alcoholic fatty liver disease. *Aliment Pharmacol Ther*. 2018;47(5):631–44.
49. Younossi ZM, Stepanova M, Rafiq N, Makhlof H, Younossi Z, Agrawal R, et al. Pathologic criteria for nonalcoholic steatohepatitis: interprotocol agreement and ability to predict liver-related mortality. *Hepatology (Baltimore, Md)*. 2011;53(6):1874–82.
50. Pavlides M, Banerjee R, Sellwood J, Kelly CJ, Robson MD, Booth JC, et al. Multiparametric magnetic resonance imaging predicts clinical outcomes in patients with chronic liver disease. *J Hepatol*. 2016;64(2):308–15.
51. Ostovaneh MR, Ambale-Venkatesh B, Fuji T, Bakhshi H, Shah R, Murthy VL, et al. Association of liver fibrosis with cardiovascular diseases in the general population: the multi-ethnic study of atherosclerosis (MESA). *Circ Cardiovasc Imaging*. 2018;11(3):e007241.
52. Gallego-Durán R, Cerro-Salido P, Gomez-Gonzalez E, Pareja MJ, Ampuero J, Rico MC, et al. Imaging biomarkers for steatohepatitis and fibrosis detection in non-alcoholic fatty liver disease. *Sci Rep*. 2016;6:31421.
53. Xie Y, Zhang H, Jin C, Wang X, Wang X, Chen J, et al. Gd-EOB-DTPA-enhanced T1 $\rho$  imaging vs diffusion metrics for assessment liver inflammation and early stage fibrosis of nonalcoholic steatohepatitis in rabbits. *Magn Reson Imaging*. 2018;48:34–41.
54. Yamada T, Obata A, Kashiwagi Y, Rokugawa T, Abe K, Matsushima S, et al. Gd-EOB-DTPA-enhanced-MR imaging in the inflammation stage of nonalcoholic steatohepatitis (NASH) in mice. *Magn Reson Imaging*. 2016;34(6):724–9.
55. Ding Y, Rao SX, Meng T, Chen C, Li R, Zeng MS. Usefulness of T1 mapping on Gd-EOB-DTPA-enhanced MR imaging in assessment of non-alcoholic fatty liver disease. *Eur Radiol*. 2014;24(4):959–66.
56. Bastati N, Feier D, Wibmer A, Traussnigg S, Balassy C, Tamandl D, et al. Noninvasive differentiation of simple steatosis and steatohepatitis by using gadoteric acid-enhanced MR



- imaging in patients with nonalcoholic fatty liver disease: a proof-of-concept study. *Radiology*. 2014;271(3):739–47.
57. Haimerl M, Utpatel K, Verloh N, Zeman F, Fellner C, Nickel D, et al. Gd-EOB-DTPA-enhanced MR relaxometry for the detection and staging of liver fibrosis. *Sci Rep*. 2017;7:41429.
  58. Haimerl M, Verloh N, Fellner C, Zeman F, Teufel A, Fichtner-Feigl S, et al. MRI-based estimation of liver function: Gd-EOB-DTPA-enhanced T1 relaxometry of 3T vs. the MELD score. *Sci Rep*. 2014;4:5621.
  59. Haimerl M, Verloh N, Zeman F, Fellner C, Muller-Wille R, Schreyer AG, et al. Assessment of clinical signs of liver cirrhosis using T1 mapping on Gd-EOB-DTPA-enhanced 3T MRI. *PLoS One*. 2013;8(12):e85658.
  60. Besa C, Bane O, Jajamovich G, Marchione J, Taouli B. 3D T1 relaxometry pre and post gadoxetic acid injection for the assessment of liver cirrhosis and liver function. *Magn Reson Imaging*. 2015;33(9):1075–82.
  61. Verloh N, Haimerl M, Zeman F, Schlabeck M, Barreiros A, Loss M, et al. Assessing liver function by liver enhancement during the hepatobiliary phase with Gd-EOB-DTPA-enhanced MRI at 3 Tesla. *Eur Radiol*. 2014;24(5):1013–9.
  62. Ding Y, Rao SXX, Zhu T, Chen CZZ, Li RCC, Zeng MSS. Liver fibrosis staging using T1 mapping on gadoxetic acid-enhanced MRI compared with DW imaging. *Clin Radiol*. 2015.
  63. Haimerl M, Verloh N, Zeman F, Fellner C, Nickel D, Lang SA, et al. Gd-EOB-DTPA-enhanced MRI for evaluation of liver function: comparison between signal-intensity-based indices and T1 relaxometry. *Sci Rep*. 2017;7:43347.
  64. Tomita K, Kikuchi M, Teratani T, Suzuki T, Taguchi T, Hibi T, et al. Evaluating the severity of nonalcoholic steatohepatitis with superparamagnetic iron oxide-enhanced magnetic resonance imaging. *J Magn Reson Imaging*. 2008;28(6):1444–50.
  65. Smits LP, Coolen BF, Panno MD, Runge JH, Nijhof WH, Verheij J, et al. Noninvasive differentiation between hepatic steatosis and steatohepatitis with MR imaging enhanced with USPIOs in patients with nonalcoholic fatty liver disease: a proof-of-concept study. *Radiology*. 2016;278(3):782–91.
  66. Bihan DL, Breton E, Lallemand D, Grenier P, Cabanis E, Laval-Jeantet M. MR imaging of intravoxel incoherent motions: application to diffusion and perfusion in neurologic disorders. *Radiology*. 1986;161(2):401–7.
  67. Parente DB, Rodrigues RS, Paiva FF, Oliveira Neto JA, do Brasil PE, Machado-Silva L, et al. Intravoxel incoherent motion diffusion weighted MR imaging at 3.0 T: assessment of steatohepatitis and fibrosis compared with liver biopsy in type 2 diabetic patients. *PLoS One*. 2015;10(5):e0125653.
  68. Murphy P, Hooker J, Bydder M, Middleton M, Sirlin C, Ang B, et al. Associations between histologic features of Nonalcoholic Fatty Liver Disease (NAFLD) and quantitative diffusion-weighted MRI measurements in adults. *J Magn Reson Imaging*. 2015;41(6):1629–38.
  69. Hansmann J, Hernando D, Reeder SB. Fat confounds the observed apparent diffusion coefficient in patients with hepatic steatosis. *Magn Reson Med*. 2013;69(2):545–52.
  70. Poyraz AK, Onur MR, Kocakoc E, Ogur E. Diffusion-weighted MRI of fatty liver. *Journal of Magn Reson Imaging*. 2012;35(5):1108–11.
  71. Guiu B, Petit JM, Capitan V, Aho S, Masson D, Lefevre PH, et al. Intravoxel incoherent motion diffusion-weighted imaging in nonalcoholic fatty liver disease: a 3.0-T MR study. *Radiology*. 2012;265(1):96–103.
  72. Leitao HS, Doblaz S, d'Assignies G, Garteiser P, Daire JL, Paradis V, et al. Fat deposition decreases diffusion parameters at MRI: a study in phantoms and patients with liver steatosis. *Eur Radiol*. 2013;23(2):461–7.
  73. Le Bihan D, Ichikawa S, Motosugi U. Diffusion and intravoxel incoherent motion MR imaging-based virtual elastography: a hypothesis-generating study in the liver. *Radiology*. 2017;285(2):609–19.